Chesapeake BAY CROSSING STUDY
TIER 2 NEPA

HYDRODYNAMICS REPORT

Maryland Transportation Authority
MDTA

MAY 2026

TABLE OF CONTENTS

1 BACKGROUND 1
2 METHODOLOGY 2
2.1 Model Approach 2
2.2 Model Setup 3
2.3 Structure Representation 5
2.4 Boundary Conditions 9
2.4.1 Tides 9
2.4.2 Wind 9
2.4.3 River Discharge 9
2.5 Model Calibration 9
3 RESULTS 13
3.1 Scenarios Evaluated 13
3.2 Velocity Magnitude 14
3.3 Shear Stress 17
4 ENVIRONMENTAL IMPACTS 20
4.1 Velocity and Shear Stress Differences 20
4.2 Potential Impacts to Sediment Transport 25
4.3 Duration of Impact 26
4.4 Summary 27
5 REFERENCES 28

LIST OF FIGURES

Figure 1. Model boundary and observation points 4
Figure 2. Existing bridge pier alignment represented in the model. 7
Figure 3. MDTA RPA bridge pier alignment represented in the model. 8
Figure 4. Tide Calibration 11
Figure 5. Velocity Calibration U-Velocity Component 12
Figure 6. Velocity Calibration V-Velocity Component 12
Figure 7. Peak velocities throughout the model domain during a flood tide at 8:30 AM on 07/03/2025 for existing bridge conditions. 15
Figure 8. Peak velocities throughout the model domain during a flood tide at 8:30 AM on 07/03/2025 for Build Alternative C conditions 15
Figure 9. Peak velocities throughout the model domain during a flood tide at 8:30 AM on 07/03/2025 for existing bridge conditions in 2100. 16
Figure 10. Peak velocities throughout the model domain during a flood tide at 8:30 AM on 07/03/2025 for Build Alternative C conditions in 2100. 16
Figure 11. Peak shear stress during a flood tide at 8:30 AM on 07/03/2025 for existing bridge conditions. 18

Figure 12. Peak shear stress during a flood tide at 8:30 AM on 07/03/2025 for Build Alternative C conditions. 18
Figure 13. Peak shear stress during a flood tide at 8:30 AM on 07/03/2025 for existing bridge conditions in 2100. 19
Figure 14. Peak shear stress domain during a flood tide at 8:30 AM on 07/03/2025 for Build Alternative C conditions in 2100. 19
Figure 15. Location of observation points. 20
Figure 16. Time series comparison at a point within the main channel (Observation Point 1) for existing and Build Alternative C pier configuration. 21
Figure 17. Time series comparison at a point 0.3 miles beyond the main channel bridge span (Observation Point 2) for existing and Build Alternative C pier configuration. 22
Figure 18 Time series comparison of shear stress at a point within the main channel (Observation Point 1) for existing and Build Alternative C pier configuration. 23
Figure 19 Time series comparison of shear stress at a point within the main channel (Observation Point 1) for existing and Build Alternative C pier configuration in future conditions. 23
Figure 20 Time series comparison of shear stress at a point within the main channel (Observation Point 2) for existing and Build Alternative C pier configuration. 24
Figure 21 Time series comparison of shear stress at a point within the main channel (Observation Point 2) for existing and Build Alternative C pier configuration in future conditions. 24
Figure 22. Mapped sediment layers 26

LIST OF TABLES

Table 1. Data Sources 5
Table 2. Water level calibration statistics 10

1 BACKGROUND

This modeling study assesses the hydrodynamics of the existing Bay Bridge area and proposed conditions of the Build Alternative C alignment identified in the Chesapeake Bay Crossing Study: Tier 2 NEPA (Tier 2 Study). The hydrodynamic model was used to evaluate flow patterns, tidal dynamics, and water level fluctuations under present-day and future (i.e., 2100) scenarios. By simulating existing and Build Alternative C conditions, the study provides an understanding of how infrastructure modifications may alter hydrodynamic processes in this region of the Chesapeake Bay.

The Chesapeake Bay is the largest estuary in the United States and is characterized by its complex interaction of tidal forcing from the Atlantic Ocean and freshwater inflows. These processes drive spatial and temporal variability in currents, which impact natural systems (e.g., sediment transport, benthic habitat) and influence human activities (e.g., navigation).

Characterization of these hydrodynamic processes is therefore important for the design and resilience of future bridge infrastructure to recognize potential adverse impacts. This hydrodynamics modeling study supports informed decision-making for the Tier 2 Study and contributes to broader coastal management and climate adaptation planning in the Chesapeake Bay.

2 METHODOLOGY

The methodology applied in this study was designed to evaluate hydrodynamic conditions in the vicinity of the Bay Bridge under existing and future build scenarios. A three-dimensional numerical modeling framework was implemented to simulate tidal circulation, water level variations, and flow velocities in the study area. The Delft3D Flexible Mesh (FM) Suite was selected for this analysis because of its capability to represent estuarine systems influenced by tides, winds, freshwater inflows, and complex shoreline geometries.

2.1 Model Approach

The 3-D hydrodynamic analysis conducted for this study utilized the D-Flow module within the Delft 3D Flexible Mesh (FM) Suite (Delft FM) (Version 2021.05). Delft FM D-FLOW, a three-dimensional (3D) hydrodynamic model, is a product of Deltares. This model solves the depth-averaged continuity equation (Equation 1) by employing the Navier Stokes equations for an incompressible fluid, incorporating Boussinesq and shallow water approximations (Equations 2 - 4). The continuity equation emerges from mass conservation while the Navier Stokes equations emerge from momentum conservation. Consistent with shallow water approximations, the model neglects vertical accelerations, simplifying the momentum conservation in the vertical direction to the hydrostatic pressure equation (Equation 4).

$$\boldsymbol{Q = \int_0^h (q_{in} - q_{out})\, dz + P - E} \quad (1)$$

Where Q represents fluxes in and out of a control volume; h is depth of the fluid with respect to mean surface level; q_{in} and q_{out} are local sources and sinks, respectively, of water per unit volume; P_{precip} is the non-local source term of precipitation; and E is the non-local sink term due to evaporation.

$$\frac{\partial u}{\partial t} + u\frac{\partial u}{\partial x} + v\frac{\partial u}{\partial y} + w\frac{\partial u}{\partial z} - fv = -\frac{1}{\rho_0}\frac{\partial P}{\partial x} + F_x + \frac{\partial}{\partial z}\left(v_V \frac{\partial u}{\partial z}\right) + M_x \quad (2)$$

$$\frac{\partial v}{\partial t} + u\frac{\partial v}{\partial x} + v\frac{\partial v}{\partial y} + w\frac{\partial v}{\partial z} - fu = -\frac{1}{\rho_0}\frac{\partial P}{\partial y} + F_y + \frac{\partial}{\partial z}\left(v_V \frac{\partial v}{\partial z}\right) + M_y \quad (3)$$

$$\frac{\partial P}{\partial z} = -\rho g h \quad (4)$$

Where u and v represent the velocity components of a fluid parcel in the x and y directions, respectively; f is the Coriolis parameter (dependent on latitude and the angular speed of the rotation of the Earth); ρ_0 is density of the incompressible fluid; P is pressure; F_x and F_y are forces emerging from any unbalanced Reynolds stresses; v_V is the vertical eddy viscosity coefficient; and M_x and M_y are moments imposed via momentum sources or sinks onto the fluid.

The above equations are applied to a spatially and temporally discretized region of interest. The spatial discretization relies on a finite volume (FV) approach, and the temporal discretization employs a finite difference (FD) method. The volumes used for spatial discretization are defined by a generated mesh. The Delft FM D-FLOW model marches through each element of the mesh to produce solutions, starting with the boundary conditions.

Four key boundary conditions characterize model performance. The kinematic boundary condition maintains the impermeability of the free surface and bottom (i.e. fluid particles on the

surface remain on the surface, and vice versa). The bed boundary condition defines components of the bed stress due to flow and waves. The surface boundary condition defines stress at the free surface as induced by winds.

D-FLOW is particularly suitable for wind- and tide-dominated flows, such as those encountered in coastal applications, and it accommodates various inputs for boundary conditions and hydrodynamic forcings. These inputs include tidal harmonic forcing, specified elevation and/or velocity time-series, surface stresses (wind and/or wave radiation stresses), slip or no-slip boundary conditions, and atmospheric pressure. Key parameters guiding the hydrodynamic model include water levels and bed bathymetry, bed roughness, wind forcing, and tidal harmonics.

Temperature and salinity dynamics were not incorporated into the model for several reasons, one of which is the limitations of the three-dimensional Delft3D FM version (2021.05) applied in this study, which does not support three-dimensional temperature and salinity boundary conditions. Also, the primary forces that drive the hydrodynamics in the Chesapeake Bay (i.e., tides, wind, and river discharge), were represented in the model. Excluding temperature and salinity reduces model complexity while still capturing the processes that determine how the Build Alternative C structural changes influence hydrodynamic behavior. While these density-driven parameters can influence circulation in estuarine systems, the primary objective of this study was to assess relative differences between existing and Build Alternative Cs under consistent forcing. This focus on the comparative changes aligns with this modeling study's objectives to highlight the relative differences in system response rather than provide absolute predictions of stratification or hydrodynamics.

2.2 Model Setup

The Delft3D model domain extended from 76.586W to 72.807W and from 38.077N to 39.665N, as shown in **Figure 1**. The model domain captured the Chesapeake Bay from upstream of the Potomac River to the Susquehanna River and incorporated the Susquehanna River up to the Conowingo Dam. The shoreline of the model domain was developed with recent shoreline data from the Maryland Department of Natural Resources (MDNR), which was projected into the geographic coordinate system World Geodetic System (WGS) 1984. The model grid domain has a minimum horizontal resolution of approximately 100 meters and a maximum of 1 kilometer, with finer resolution near the Bay Bridge and along the Susquehanna River.

Figure 1. Model boundary and observation points



The bathymetry sources include recent U.S. Army Corps of Engineers (USACE) hydrographic survey data incorporated in the Chesapeake Bay Topobathymetric DEM (TBDEM), with surveys extending through 2015, and more recent navigation channel condition monitoring by the USACE

Baltimore District documented as late as 2023. With respect to the vertical distribution, a 6 sigma-layer distribution was implemented. The number of layers was selected to balance computational efficiency and representation of conditions. Model elevations were with respect to the NAVD88 vertical datum.

This study used public environmental data to develop and calibrate the hydrodynamic model. Tidal data from two National Oceanic and Atmospheric Administration (NOAA) Operational Oceanographic Products and Services (CO-OPS) stations were used to develop tidal boundary conditions. Wind speed, wind direction, and atmospheric pressure data from five NOAA National Data Buoy Center (NDBC) stations were used to develop wind boundary conditions for the hydrodynamic model.

Finally, a discharge boundary condition at the Susquehanna River was developed using discharge data collected by the United States Geological Survey (USGS). Five NOAA tidal stations were used to calibrate the model. Three NOAA current prediction stations and observation data from two NOAA active current stations were used. The stations used to develop the hydrodynamic model boundary conditions and calibrate the model are presented in **Table 1** and **Figure 1**.

Table 1. Data Sources

Type of Station	Application	Station Name	Longitude (°W)	Latitude (°N)
Tidal Elevation	Boundary Condition	NOAA 8571421	76.04	38.22
		NOAA 8573927	75.81	39.53
	Model Calibration	NOAA 8573927	-75.81	39.53
		NOAA 8573364	-76.24	39.21
		NOAA 8574680	-76.58	39.27
		NOAA 8571421	-76.04	38.22
		NOAA 8575512	-76.48	38.98
River Discharge	Boundary Condition	USGS 01578310	-76.17	39.66
Current Measurement	Model Calibration	cb1001	-76.38	38.40
		cb1101	-76.38	38.98
		CHB0301	-76.27	38.30
		CHB0302	-76.30	39.07
		CHB0304	-76.36	38.49
Wind Measurement	Boundary Condition	NDBC tcbm2	76.24	39.21
		NDBC tplm2	76.44	38.90
		NDBC fskm2	76.53	39.22
		NDBC 44062	76.42	38.56
		NDBC 44063	76.45	38.96

2.3 Structure Representation

In the Delft3D model, structures were represented by 'thin dams' for both existing conditions (**Figure 2**) and the Build Alternative C conditions (**Figure 3**). Representation of these structures required the specification of grid cells where flow was restricted or blocked to approximate the physical location of bridge piers. For the Build Alternative C conditions, new pier placements and

changes to span spacing were explicitly encoded into the model grid to accurately capture the hydraulic influence of these structures on surrounding flow fields. Other structures represented in the model by thin dams included shoreline stabilization features (e.g., groins, jetties), which were similarly implemented by modifying the grid and applying appropriate flow resistance parameters.

The existing Bay Bridge consists of multiple spans with pier spacing that varies by bridge segment, with wider openings across the main navigation channel and narrower spacing near approach structures. These varying pier spacings were represented explicitly in the model geometry to reflect bridge spans. The Build Alternative C scenario was designed to be representative of Build Alternative C pier locations and span widths. The pier outlines represented in the model are intended to reflect the maximum anticipated limits of disturbance associated with the conceptual bridge design and were selected conservatively as a 'worst-case' for the purposes of the hydrodynamic analysis. As design advances, actual constructed pier footings will be smaller than those represented in the model.

As shown in the existing conditions figure (**Figure 2**), span widths in the eastern portion of the bridge are narrow, with average openings on the order of approximately 70 to 120 feet, gradually increasing to spans of roughly 300 to 460 feet moving toward the central portion of the crossing. Within the central section of the bridge, existing spans increase substantially but remain segmented by multiple intermediate piers, with the main channel spanning approximately 1,950 feet. Toward the western side of the bridge, span widths decrease again, with openings less than 100 feet.

The limits of disturbance that are represented in the Build Alternative C mostly decrease the span width between piers. As shown in the Build Alternative C figure (**Figure 3**), spans in the eastern section of the bridge increase from existing widths of less than 120 feet to openings ranging from approximately 280 to 420 feet. Across the central portion of the crossing, the Build Alternative C includes longer spans, with individual openings from east to west on the order of approximately 1,500 feet and 800 feet, and fewer intermediate piers compared to existing conditions. In the western section, typical span lengths increase to approximately 340 to 360 feet, with shorter openings near the abutments. This configuration overall reduces span widths as compared to the existing conditions.

To adequately resolve flow between bridge piers for both scenarios, the model grid was constructed to maintain a minimum of five computational cells between adjacent piers for both existing and Build Alternative C conditions. This resolution threshold of the model maintains sufficient representation without excessive computational demands. Grid spacing between piers was refined, as needed, to satisfy this minimum requirement while maintaining overall numerical stability and computational efficiency.

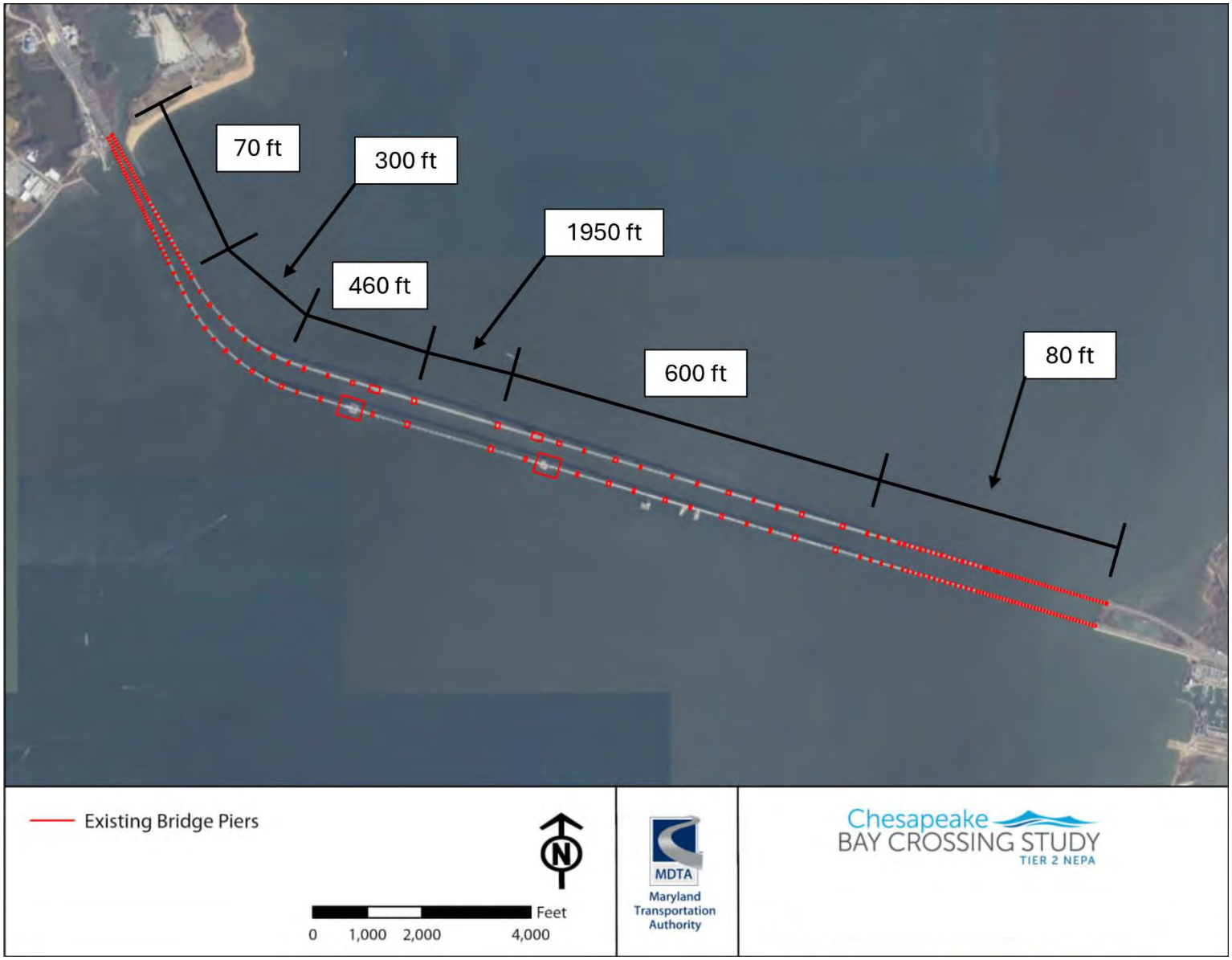


Figure 2. Existing bridge pier alignment represented in the model.

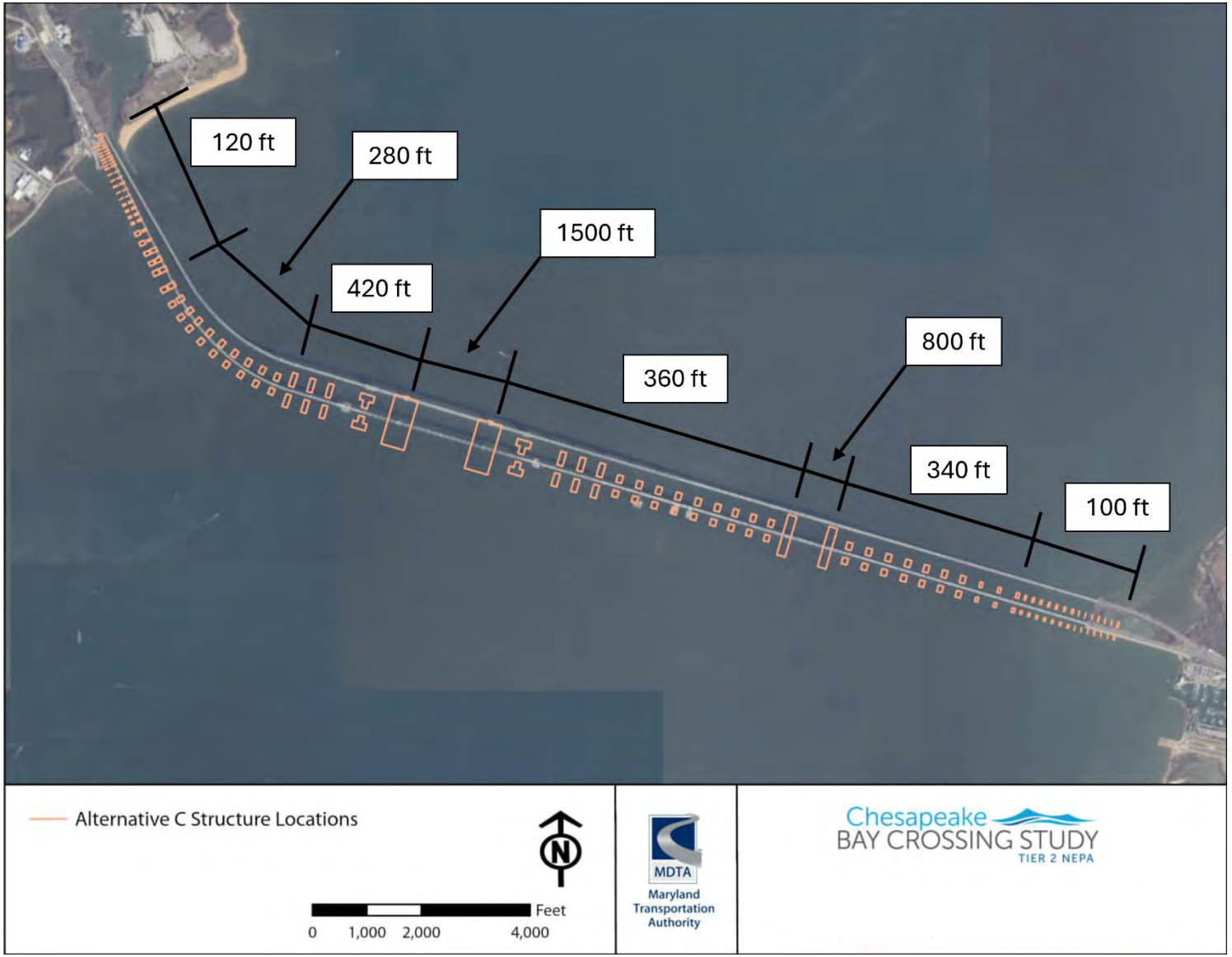


Figure 3. MDTA RPA bridge pier alignment represented in the model.

2.4 Boundary Conditions

Boundary conditions were developed to represent the dominant physical processes controlling hydrodynamics in the Bay Bridge study area. Tidal water levels, wind forcing, and river discharge were applied to the model using observational datasets to maintain realistic representation of circulation patterns, water level variability, and flow velocities. The following sections describe how each condition was prescribed in the model.

2.4.1 Tides

Water levels were prescribed as a function of time at the two tidal boundary conditions using 6-minute observation data from NOAA (**Figure 1**). In Delft3D FM, tidal boundary conditions are typically defined by specifying water level time series at open boundaries of the computational domain, which then propagate inward through the model according to the governing hydrodynamic equations. The use of high-frequency (6-minute) NOAA observations resolves the tidal variability, including higher-frequency fluctuations such as tidal asymmetry and spring-neap modulation. For future conditions, water level forcings were adjusted to incorporate projected sea level change consistent with the NOAA (2022) Intermediate-High scenario. Under this scenario, water levels in the Chesapeake Bay are forecasted to increase by approximately 3.5 feet by 2100. This offset was applied uniformly to the tidal boundary water level time series to represent elevated future water levels. No changes were made to the tidal harmonic constituents themselves; instead, the future scenario assumes that tidal forcing at the open boundaries remains identical to present-day conditions aside from the vertical water level offset. As water levels rise, the position of wet cells in the Delft3D-FM mesh adjusts dynamically, allowing inundation of low-lying areas to be represented within the computational domain.

2.4.2 Wind

Atmospheric pressure and u- and v-components of wind speed were applied to the model based on 6-minute observation data from NOAA. In Delft3D FM, wind and pressure boundary conditions are incorporated as surface forcing terms that act directly on the free surface and influence circulation patterns throughout the domain. The use of 6-minute observational data allowed for the accurate representation of short-term variability in wind forcing, such as gusts and directional shifts, as well as barometric pressure changes associated with passing weather systems.

2.4.3 River Discharge

The discharge boundary condition at the Susquehanna River was prescribed using 15-minute flow data obtained from the USGS monitoring station at Conowingo Dam. This dataset captures the temporal variability of river discharge, including short-term fluctuations driven by precipitation events and reservoir operations. The Susquehanna discharge was applied at the upstream river boundary as a flow rate time series. Discharges from smaller tributaries entering the Chesapeake Bay were not explicitly included in the model, as their contributions are small relative to the dominant tidal forcing.

2.5 Model Calibration

The model roughness coefficient was calibrated to maintain the accuracy and reliability of the outputs. Calibration involves the refinement of model parameters to align with simulated and observed values, to enhance its predictive capabilities. Bottom roughness represents the resistance to flow within the water body and is directly related to flow velocities and distributions. The calibration process involved adjusting the values of roughness based on bottom substrate to achieve the best agreement between simulated and observed flow velocities. Coefficients were

either specified as Manning's 'n' or Chezy coefficient as part of the calibration process to evaluate which reduced error. **Table 2** summarizes quantitative calibration statistics for water level comparisons at multiple monitoring stations using different roughness values. These statistics indicate that variations in bottom roughness have a relatively small influence on water level reproduction, with all tested formulations providing strong agreement with observations. The results in **Table 2** were used to check that the chosen roughness parameters supported accurate simulation of water levels. Based on the calibration statistics summarized in **Table 2**, a Manning roughness coefficient of 0.03 was selected for subsequent simulations, as it provided the best balance of low error and consistent performance across all calibration stations.

Table 2. Water level calibration statistics

Water Level Statistics					
Location	**Station ID**	**R^2**	**RMSE (m)**	**Mean Water Level (observed) (m NAVD88)**	**Mean Water Level (modeled) (m NAVD88)**
Manning 0.023					
Tolchester Beach	8573364	0.78	0.11	0.25	0.24
Baltimore	8574680	0.77	0.11	0.26	0.24
Annapolis	8575512	0.80	0.09	0.21	0.23
Solomons Island	8577330	0.89	0.06	0.21	0.21
Manning 0.03					
Tolchester Beach	8573364	0.78	0.09	0.25	0.24
Baltimore	8574680	0.76	0.09	0.26	0.24
Annapolis	8575512	0.79	0.08	0.21	0.23
Solomons Island	8577330	0.89	0.05	0.21	0.21
Manning 0.05					
Tolchester Beach	8573364	0.73	0.10	0.25	0.24
Baltimore	8574680	0.71	0.09	0.26	0.24
Annapolis	8575512	0.75	0.07	0.21	0.23
Solomons Island	8577330	0.90	0.05	0.21	0.22
Chezy 70					
Tolchester Beach	8573364	0.77	0.11	0.25	0.24
Baltimore	8574680	0.77	0.11	0.26	0.24
Annapolis	8575512	0.81	0.09	0.21	0.23
Solomons Island	8577330	0.90	0.06	0.21	0.21

Figure 4 presents a comparison between modeled water levels at observed stations to evaluate model performance under different roughness formulations. The time series comparison demonstrates that the model reproduces both the magnitude and phase of tidal fluctuations with good agreement across the analysis period.

Figures 5 and 6 present comparisons between observed and modeled current velocities for the u and v directional components at stations used in this analysis. The time series comparisons show that the model captures the magnitude, phase, and directional variability of tidal currents with reasonable accuracy across the calibration period. The calibration results indicate that the

model adequately reproduces observed current behavior under the combined influence of tidal forcing, wind, and river discharge.

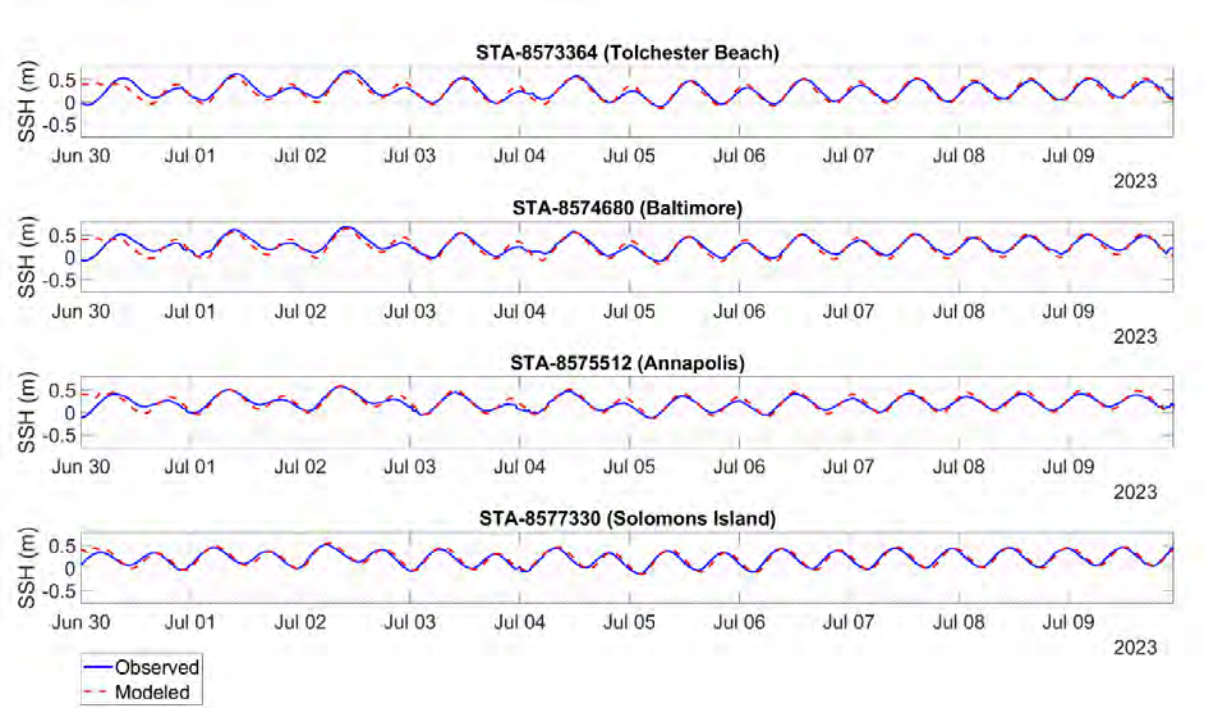


Figure 4. Tide Calibration

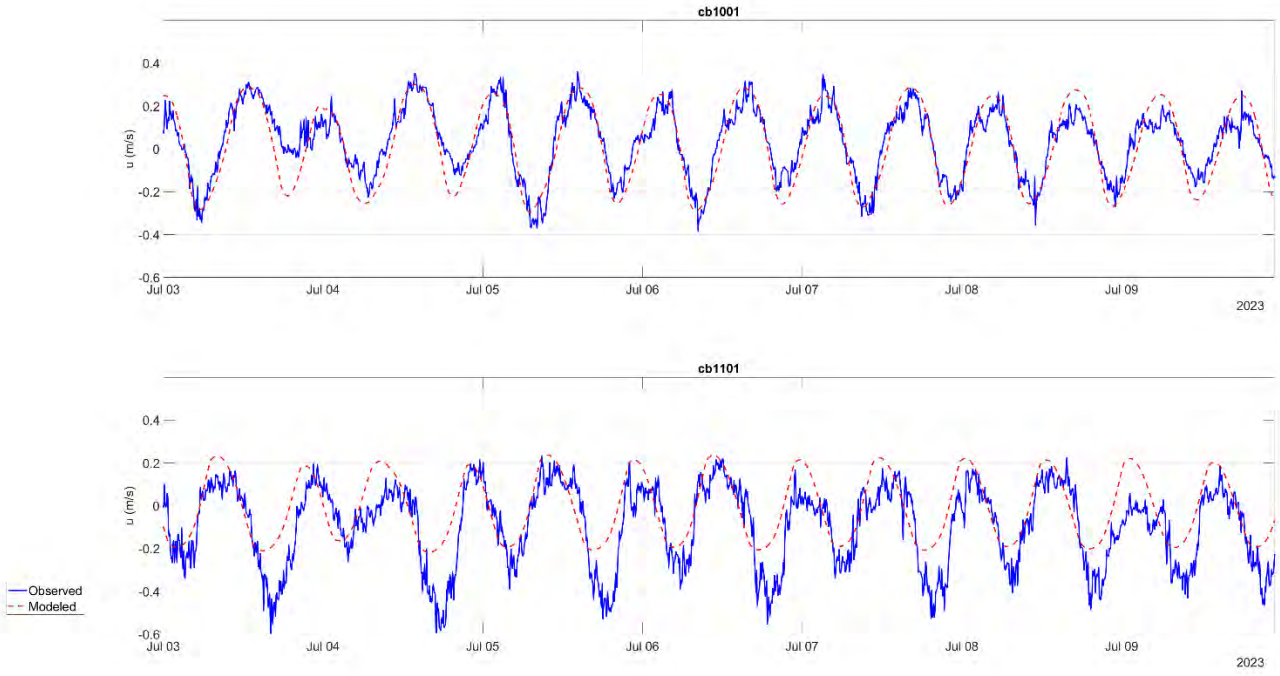


Figure 5. Velocity Calibration U-Velocity Component

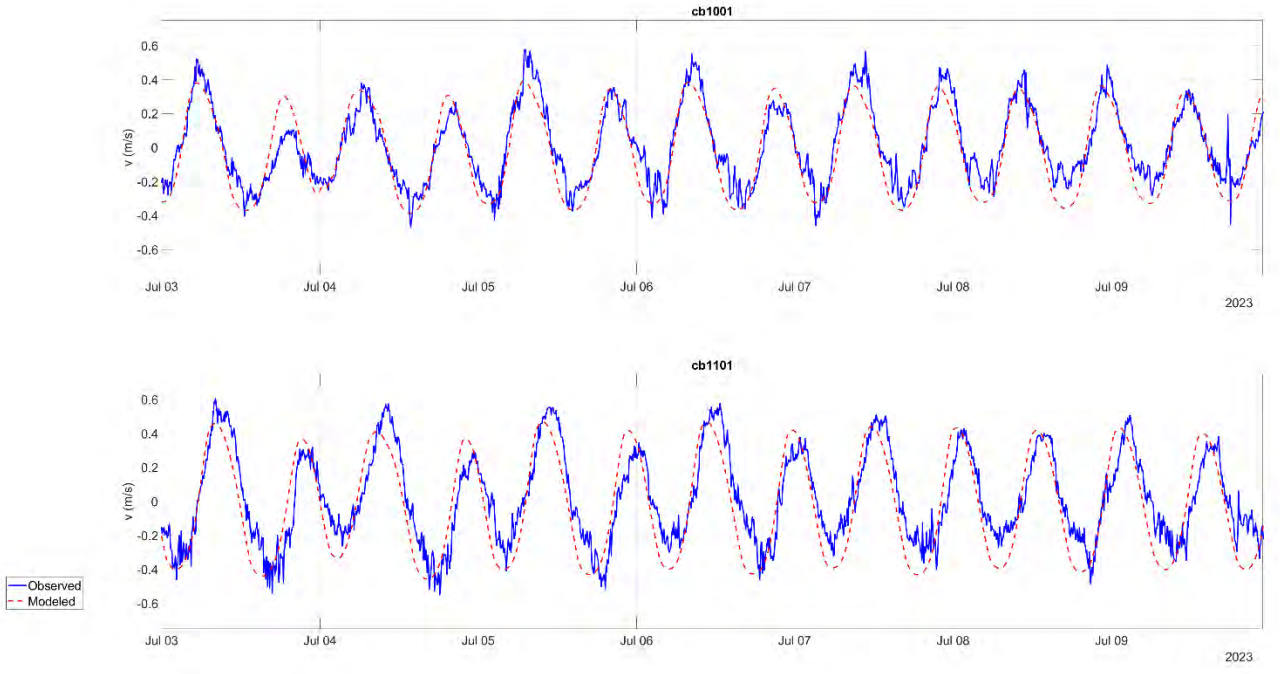


Figure 6. Velocity Calibration V-Velocity Component

3 RESULTS

The model was run for the period from June 30, 2023, to July 9, 2023, with three days of model spin-up to allow the system to stabilize prior to the analysis window. This period was selected because it encompassed large tidal swings associated with a "king" tide during the time period in which collected data were available. The assessment of this time period captured flows in which the influence of the Bay Bridge Build Alternative C may impact environmental conditions.

Analysis of observed current data at NOAA buoy CB1101, located near the Bay Bridge, indicates that the modeled flow velocity time step corresponds approximately to the 95th percentile of depth averaged velocities over a five-year observation period (2018-2023). Therefore, the simulated velocities provide a conservative basis for assessing differences between existing and Build Alternative C bridge configurations. The following sections summarize these results, highlighting differences between existing and Build Alternative C conditions.

3.1 Scenarios Evaluated

To evaluate the potential hydrodynamic impacts associated with the Bay Bridge and Build Alternative C conditions in the surrounding system, four scenarios were developed and simulated using the hydrodynamic model. A summary of each scenario and its representation in the model is provided below.

- Existing Bridge Conditions (Present Day): This scenario represents existing hydrodynamic conditions in the Bay Bridge study area. Bathymetry, shoreline configuration, and existing bridge infrastructure were represented in the model as surveyed. Boundary conditions reflect present-day tidal forcing, freshwater inflows, and meteorological conditions, providing a baseline for comparison against the Build Alternative C and future conditions.

- Build Alternative C Conditions (Present Day): The Build Alternative C conditions (present day) scenario incorporates conceptual design elements associated with bridge modifications and associated structures. These modifications include adjustments to pier placement. All other forcing conditions (tides, inflows, meteorology) are held consistent with the existing conditions scenario to isolate the influence of structural changes.

- Existing Bridge Conditions (2100): This future condition scenario reflects projected changes in hydrodynamics due to sea level change, assuming no structural modifications to the bridge beyond current conditions. This scenario allows for evaluation of how changes in environmental conditions alter tidal circulation and velocity distributions in the study area.

- Build Alternative C Conditions (2100): This scenario combines the Build Alternative C structural modifications (as described in the Build Alternative C Conditions scenario) with the projected 2100 future conditions (as described in the existing bridge conditions [2100] scenario). The representation includes modified pier and channel configurations under a higher sea level baseline. The purpose of this scenario is to assess the interaction of long-term water level change with the Build Alternative C conditions and to evaluate potential cumulative impacts on tidal hydrodynamics, specifically, to velocity magnitude.

3.2 Velocity Magnitude

Spatially varying current velocity results from the modeled existing conditions during a period of strong tidal flows are shown for the entire study area in **Figure 7**. These results depict spatial variations in current velocity across the study area with color-coded contours overlayed onto a geographic base map to show patterns of water movement and distribution during peak flow. Current velocities are more pronounced in the model domain due to the Bay's bathymetry, coastline morphology, and structures (e.g., existing Bay Bridge) which can constrict flows. Deeper channels represented by the model bathymetry exhibit stronger tidal currents, while shallower regions and tributary mouths experience reduced velocities. For example, faster currents are found in the constricted parts of the Bay (e.g., between Sandy Point and Kent Island) in the vicinity of the existing bridge.

Peak modeled velocities in the vicinity of the bridge during the simulation period were found to be consistent along the bridge channel between the piers. Under present-day water levels, average peak velocities between the bridge spans were 1.7 to 2.1 ft/s for the existing bridge piers. For the Build Alternative C, average peak velocities were higher, ranging from 2.6 (48% increase in peak velocity) to 3.1 ft/s (53% increase in peak velocity), reflecting flow constriction effects from the revised pier geometry and more conservative limits of disturbance of the Build Alternative C. These increases are consistent with higher water levels allowing for greater overall flow energy and increased velocities through the bridge channel. A velocity maximum over the entire model domain of 3.1 ft/s was found near the Sandy Point Shoal Light under present-day conditions, with higher velocities under future water levels.

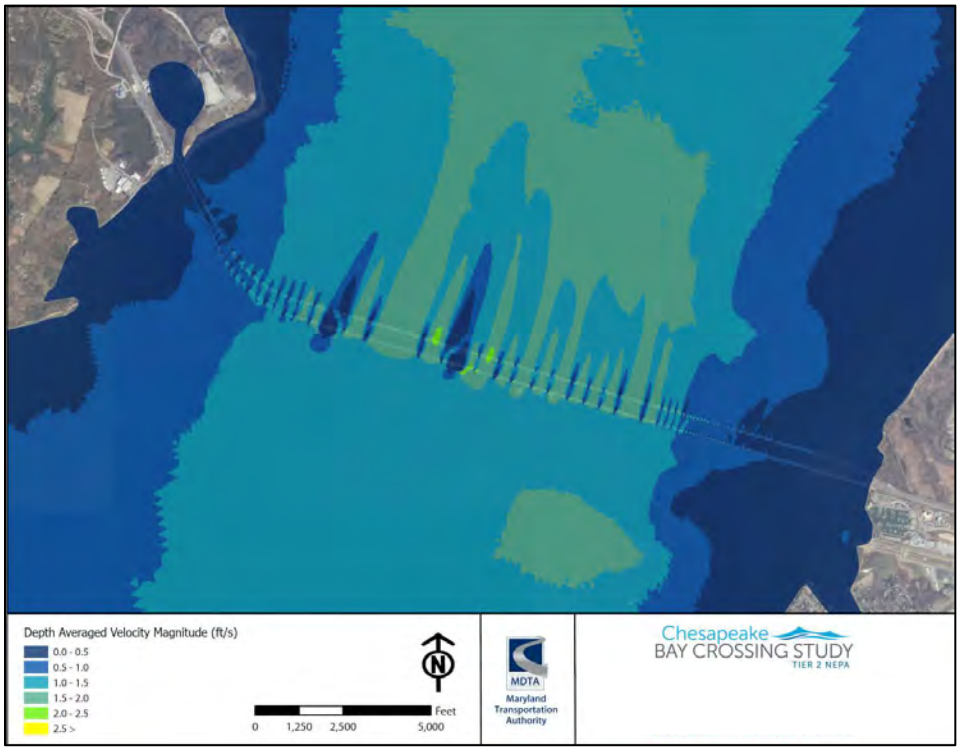


Figure 7. Peak velocities throughout the model domain during a flood tide at 8:30 AM on 07/03/2025 for existing bridge conditions.

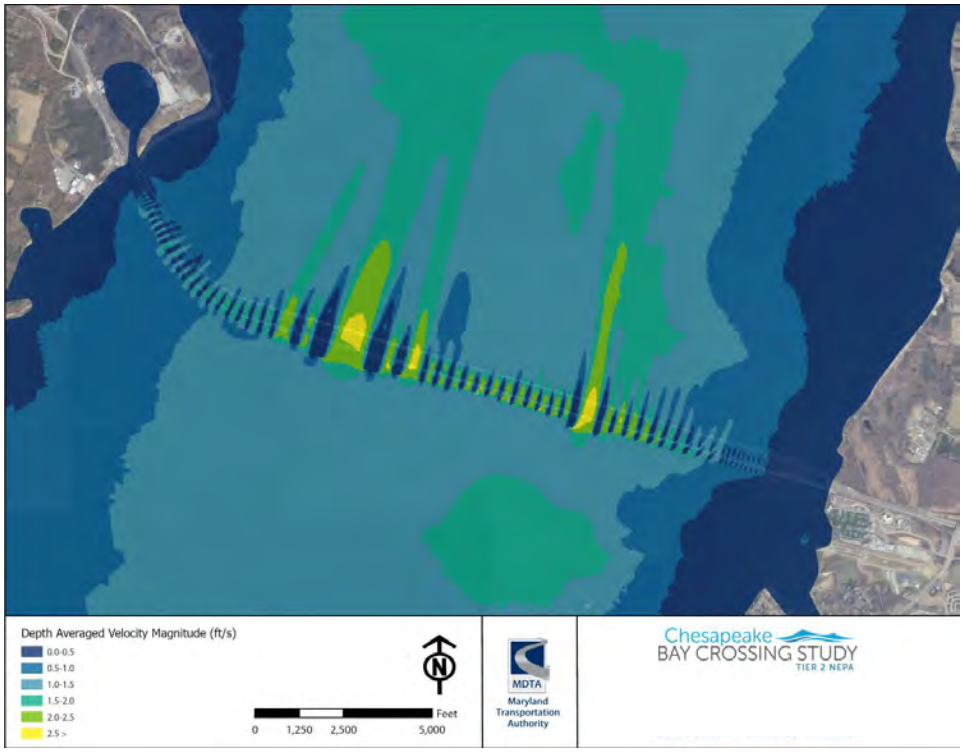


Figure 8. Peak velocities throughout the model domain during a flood tide at 8:30 AM on 07/03/2025 for Build Alternative C conditions

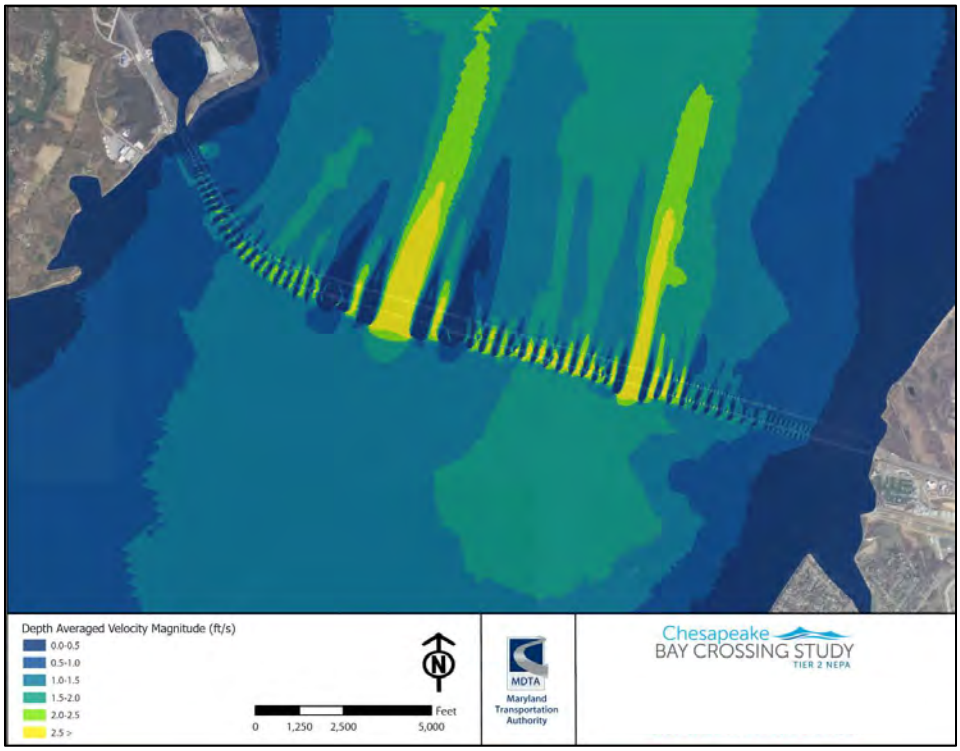


Figure 9. Peak velocities throughout the model domain during a flood tide at 8:30 AM on 07/03/2025 for existing bridge conditions in 2100.

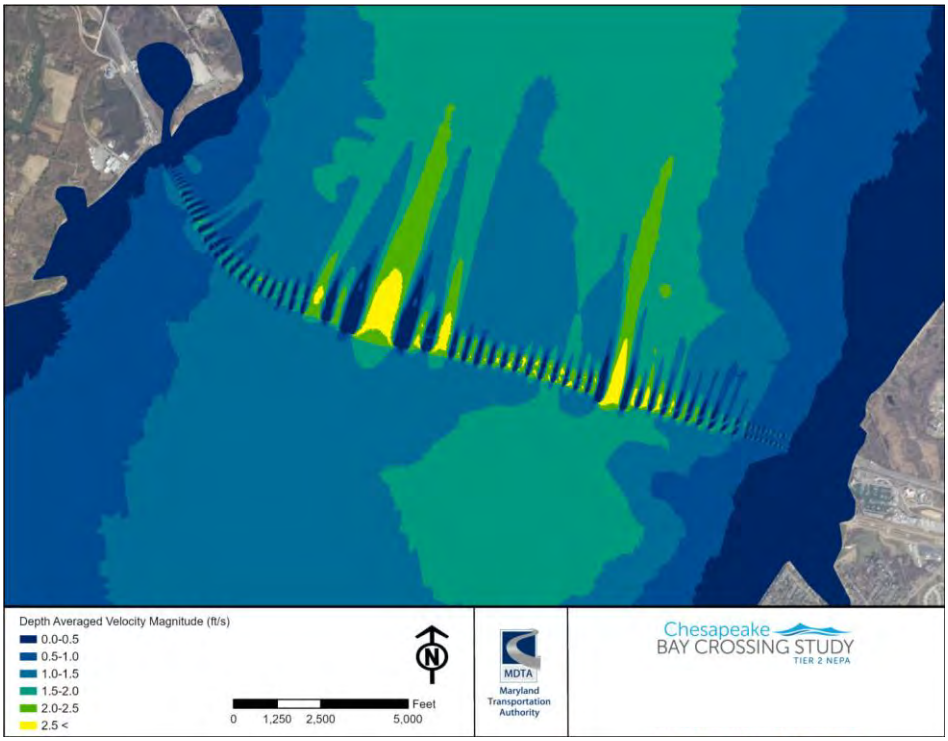


Figure 10. Peak velocities throughout the model domain during a flood tide at 8:30 AM on 07/03/2025 for Build Alternative C conditions in 2100.

3.3 Shear Stress

Modeled bottom shear stress was evaluated for existing and Build Alternative C bridge configurations for both present day and future water level conditions to assess spatial patterns of near bed forcing in the vicinity of the Bay Bridge. **Figures 7 and 8** present shear stress magnitudes during a representative period of peak tidal flow for existing and Build Alternative C bridge configurations under present day water levels, respectively. **Figures 9 and 10** show the corresponding shear stress distributions for existing and Build Alternative C conditions under future water level conditions.

Under present day conditions, shear stress patterns for the existing bridge configuration shown in **Figure 7** indicate elevated values within the main navigation channel and near bridge piers (i.e., 0.5 – 2.0 Pa), where flow acceleration occurs as tidal currents pass between spans. Lower shear stress values (i.e., < 0.1 Pa) are observed in shallower areas and farther from the bridge, where flow velocities are reduced. **Figure 8** shows shear stress results for the Build Alternative C bridge configuration under the same forcing conditions. Shear stress values are similar to those observed under existing conditions, with localized increases in shear stress between selected spans where pier spacing is reduced, and localized decreases in areas where hydraulic openings are increased relative to existing conditions.

Figures 9 and 10 illustrate shear stress distributions under future water level conditions for the existing and Build Alternative C bridge configurations. Overall shear stress magnitudes are greater than those observed under present day conditions, reflecting increased flow velocities and resulting shear stresses. Across all scenarios, changes in shear stress attributable to the Build Alternative C bridge configuration diminish rapidly with distance from the bridge, and shear stress distributions beyond the bridge vicinity are similar between existing and Build Alternative C conditions.

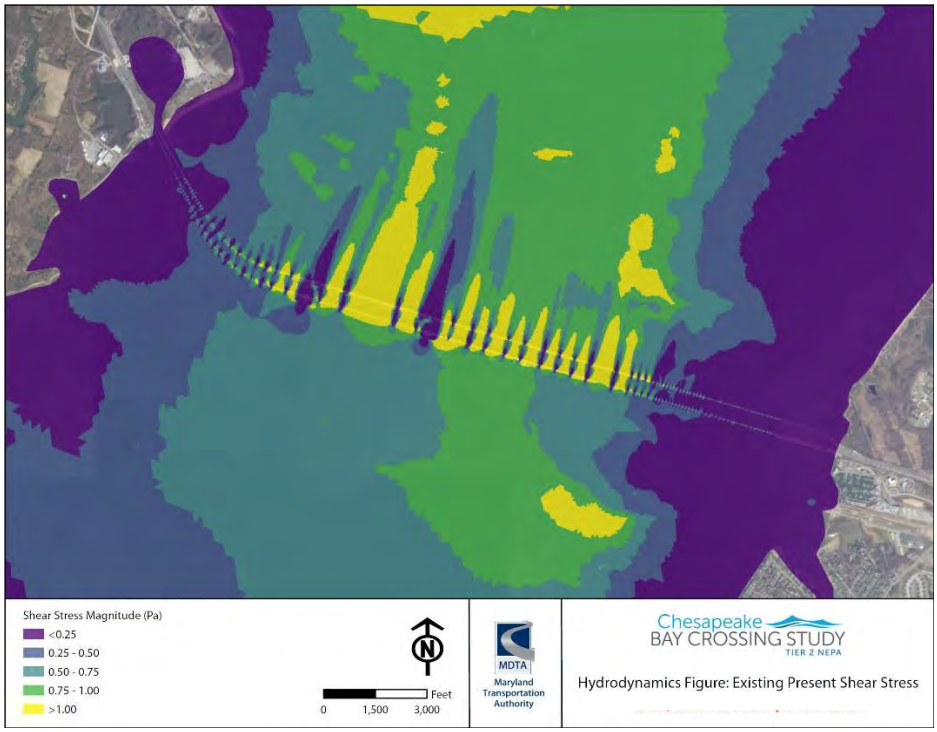


Figure 11. Peak shear stress during a flood tide at 8:30 AM on 07/03/2025 for existing bridge conditions.

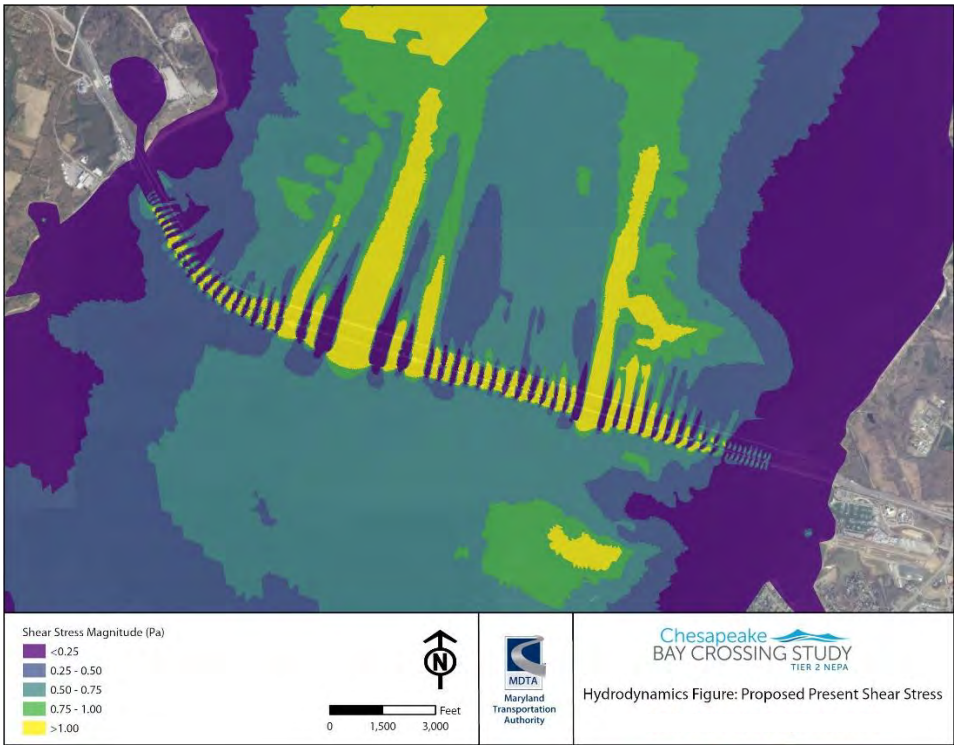


Figure 12. Peak shear stress during a flood tide at 8:30 AM on 07/03/2025 for Build Alternative C conditions.

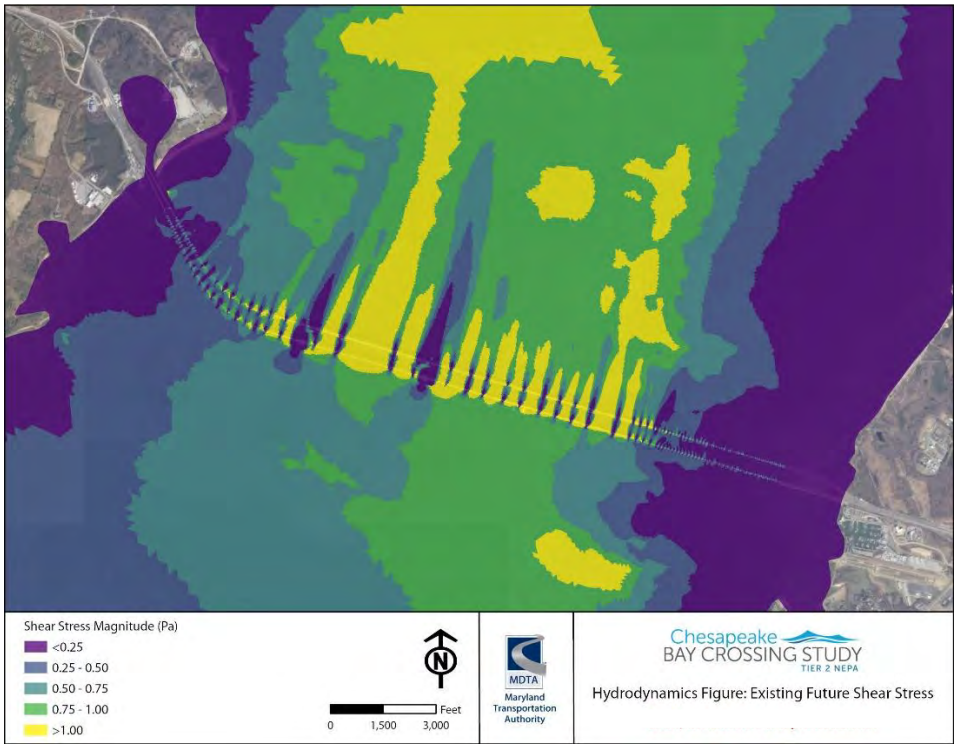


Figure 13. Peak shear stress during a flood tide at 8:30 AM on 07/03/2025 for existing bridge conditions in 2100.

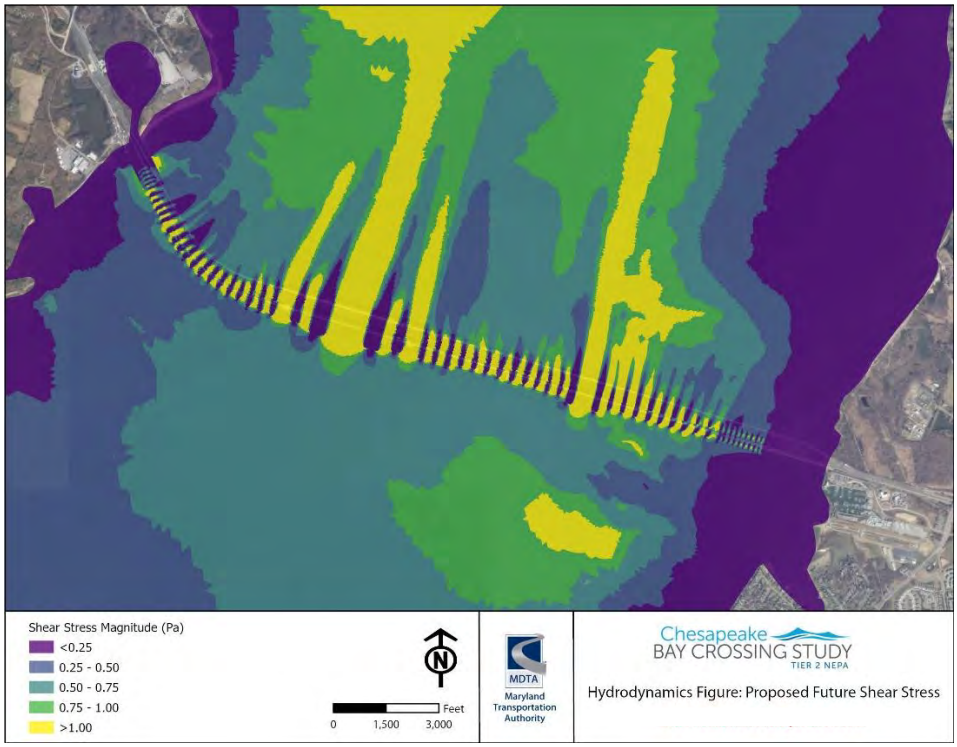


Figure 14. Peak shear stress domain during a flood tide at 8:30 AM on 07/03/2025 for Build Alternative C conditions in 2100.

4 ENVIRONMENTAL IMPACTS

The hydrodynamic model was applied to evaluate the Build Alternative C scenarios in the vicinity of the Bay Bridge relative to existing conditions. These scenarios were designed to assess how potential modifications and projected future conditions (i.e., change in water levels) could influence tidal circulation as well as velocity and shear stress distributions in the study area. Results between scenarios were compared at two representative observation points (**Figure 15**): Observation Point 1 between existing bridge spans, and Observation Point 2 0.3 miles south of the bridge. The following sections analyze differences in the results between the existing conditions and the Build Alternative C at the two observation points and their potential environmental impacts.



Figure 15. Location of observation points.

4.1 Velocity and Shear Stress Differences

Comparison of time series of flow velocities indicates that under the Build Alternative C pier configuration, peak velocities are greater (48 to 53 %) within the main channel between the bridge spans compared to existing conditions, reflecting localized flow constriction and acceleration around the new, larger pier geometry. However, these differences diminish with distance from the bridge, and approximately 0.3 miles downstream and upstream, velocities and shear stresses under the Build Alternative C conditions closely match those of the existing bridge, with velocities greater in the existing condition scenario (-2 to -4%). This pattern demonstrates that while the Build Alternative C pier configuration influence flow within the immediate channel, their effects on hydrodynamics are localized to the piers.

Modeling results indicate that differences in velocity between existing and Build Alternative C conditions are primarily driven by changes in bridge pier position and span spacing. Areas where the Build Alternative C conditions introduce narrower spans or increased pier density show localized increases in flow velocity, as the constricted spacing accelerates water moving through the channel. Conversely, locations with wider spans exhibit reduced velocities relative to existing conditions, reflecting the reduced hydraulic resistance in those areas.

These differences in velocities can be seen in Figure 16 for the bottom layer and Figure 17 for the surface layer during peak modeled flow conditions. Larger differences in velocity (48 – 53%), further from the bridge were found to be for the surface layer. The largest increases in velocity occur in the location where the main span piers from the existing bridge are removed. Some increases in velocity are also found near the abutment close to Kent Island, however these changes are mostly constrained between each bridge approach. Decreases in velocity are found near the main channel, as well as the center of the bridge span, due to the increases in span width.

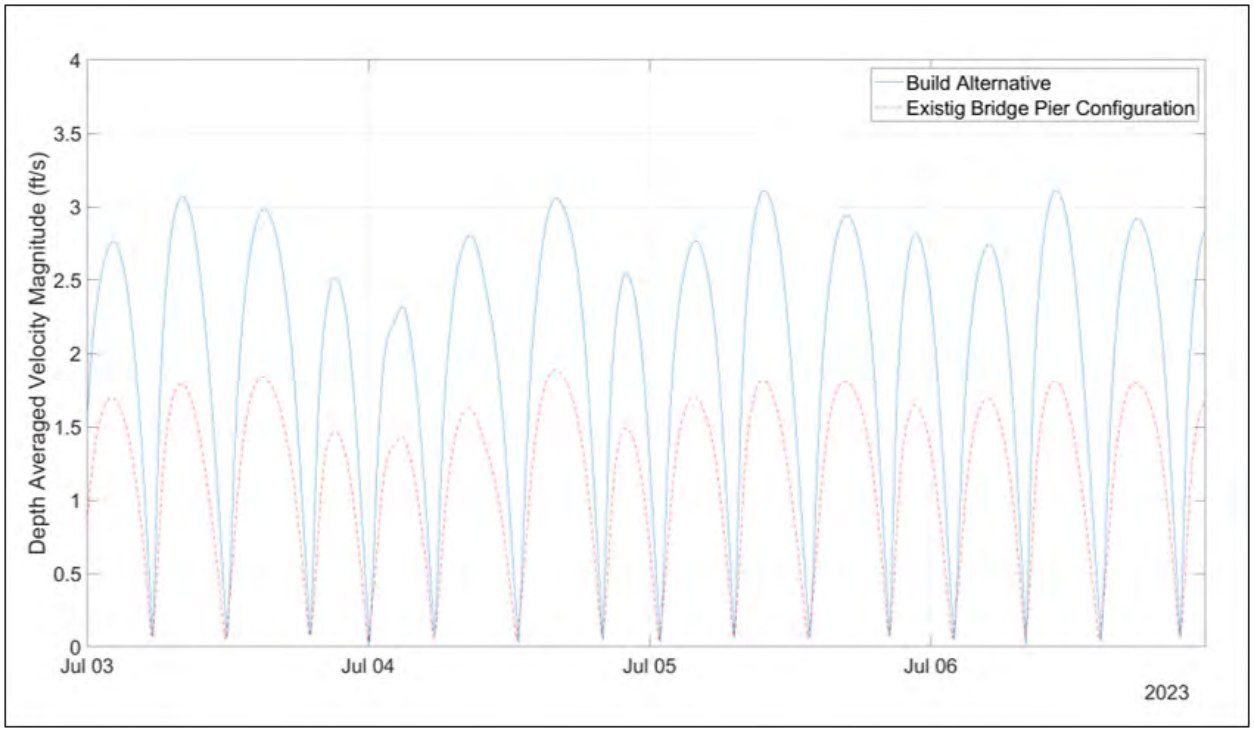


Figure 16. Time series comparison at a point within the main channel (Observation Point 1) for existing and Build Alternative C pier configuration.

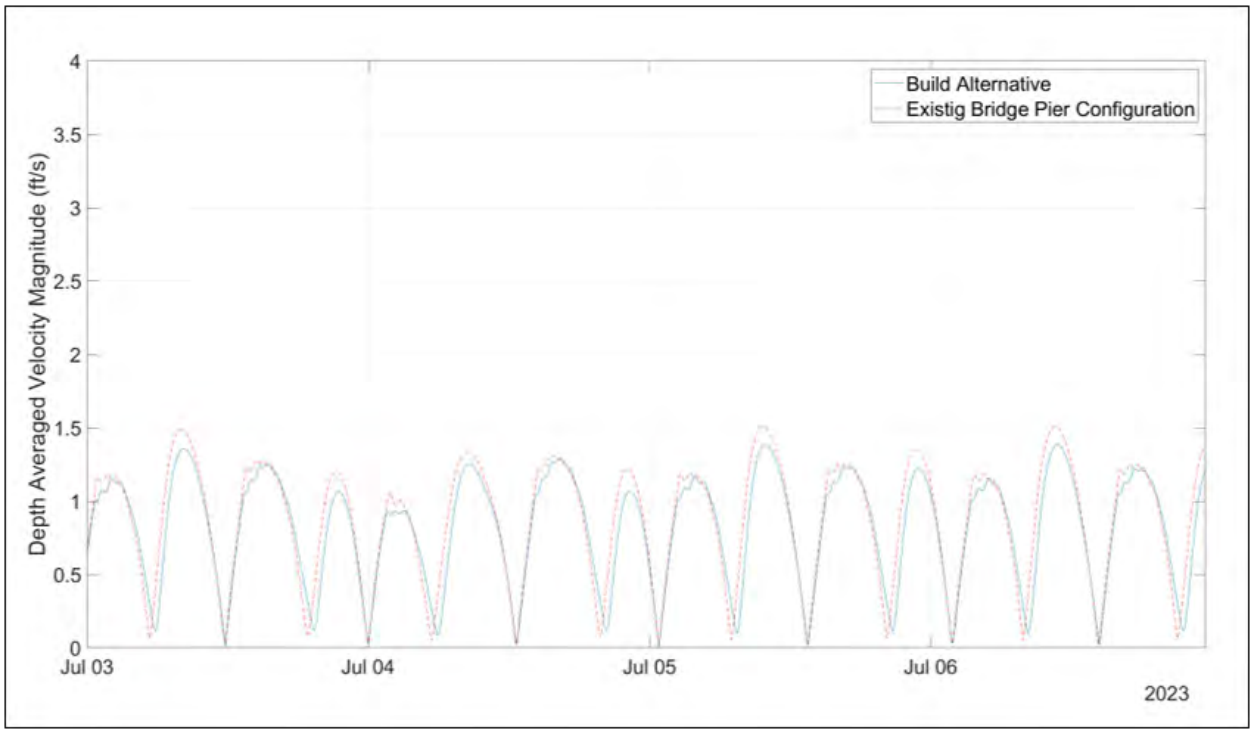


Figure 17. Time series comparison at a point 0.3 miles beyond the main channel bridge span (Observation Point 2) for existing and Build Alternative C pier configuration.

Figures 18 through 21 present time series of modeled bottom shear stress during the period surrounding peak tidal flow on July 03 for existing and proposed bridge configurations under present day and future water level conditions. Results are shown at the two representative observation points to illustrate both local and downstream effects. These figures show the temporal evolution of shear stress before, during, and after the peak flow period.

At Observation Point 1, peak shear stress values for the proposed bridge configuration are greater (10-25%) than those under existing conditions during the peak flow window. These differences are confined to a short interval around peak tidal flow and diminish rapidly as flow velocities decrease. At Observation Point 2, time series results indicate minimal differences between existing and proposed conditions, with peak shear stress values differing by less than 5%. These results demonstrate that changes in shear stress associated with the proposed bridge configuration are localized to the bridge channel and do not persist downstream.

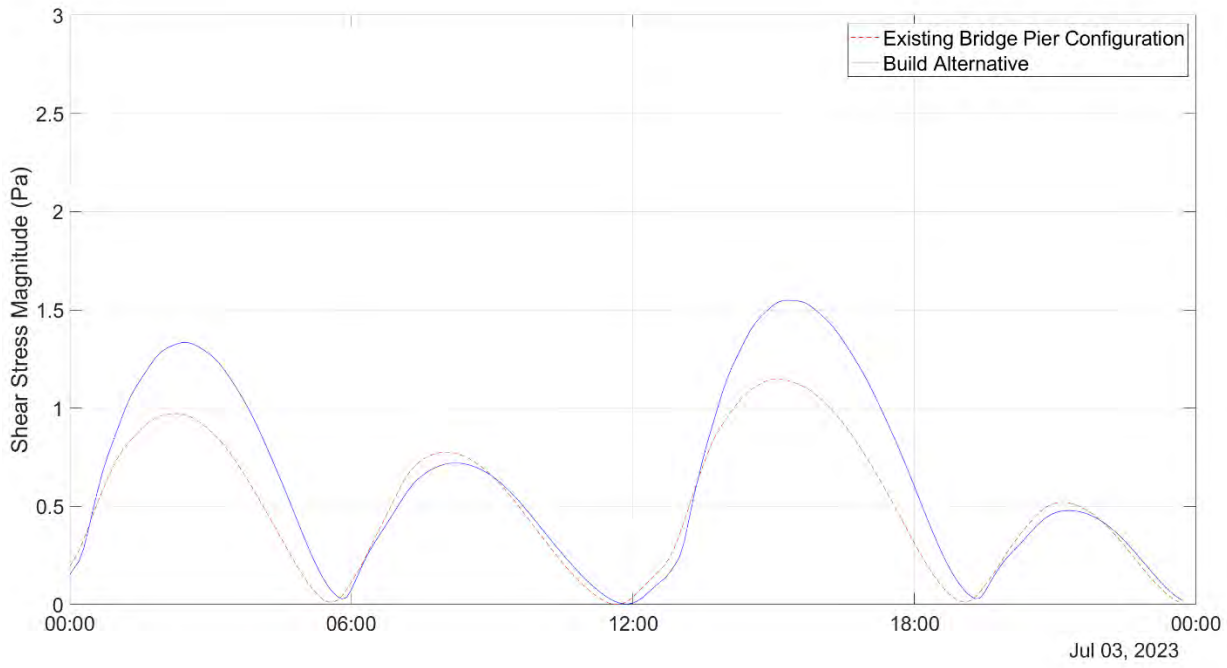


Figure 18 Time series comparison of shear stress at a point within the main channel (Observation Point 1) for existing and Build Alternative C pier configuration.

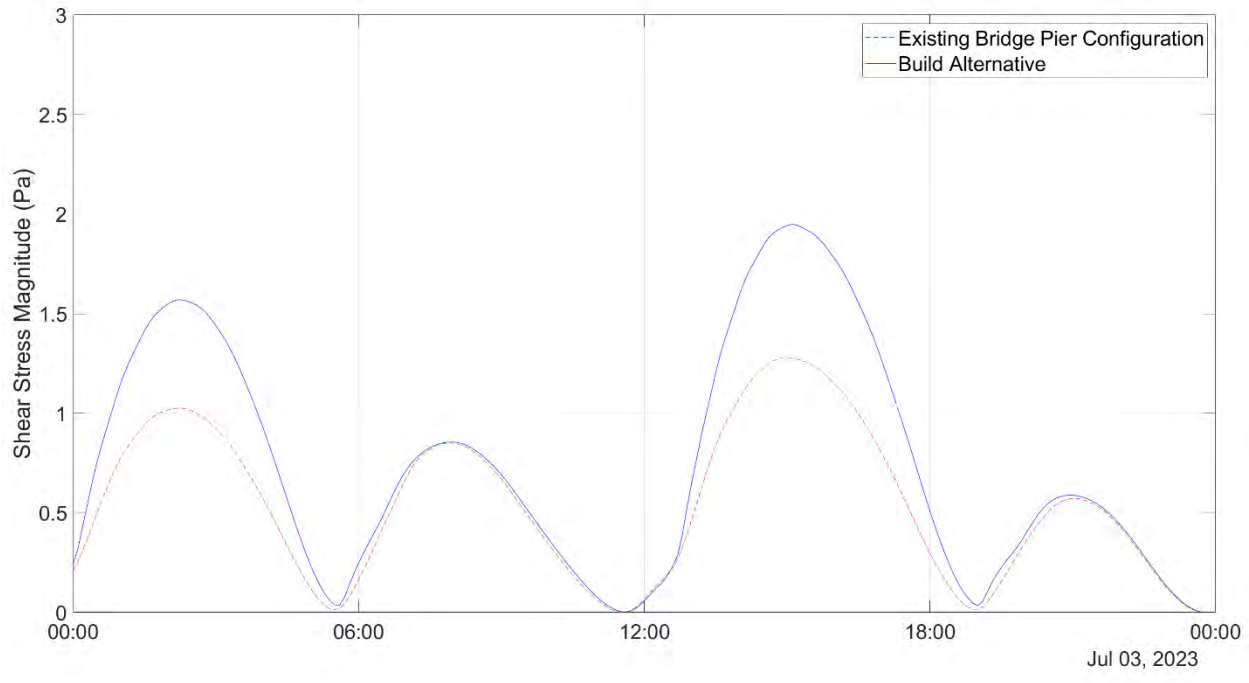


Figure 19 Time series comparison of shear stress at a point within the main channel (Observation Point 1) for existing and Build Alternative C pier configuration in future conditions.

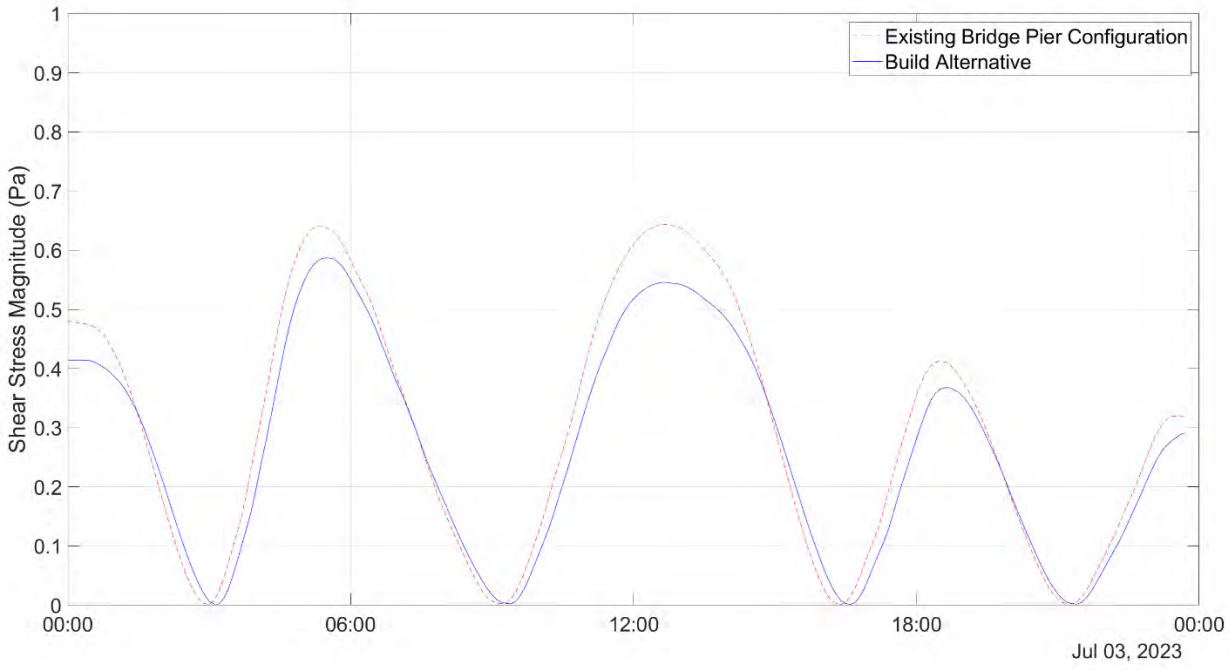


Figure 20 Time series comparison of shear stress at a point within the main channel (Observation Point 2) for existing and Build Alternative C pier configuration.

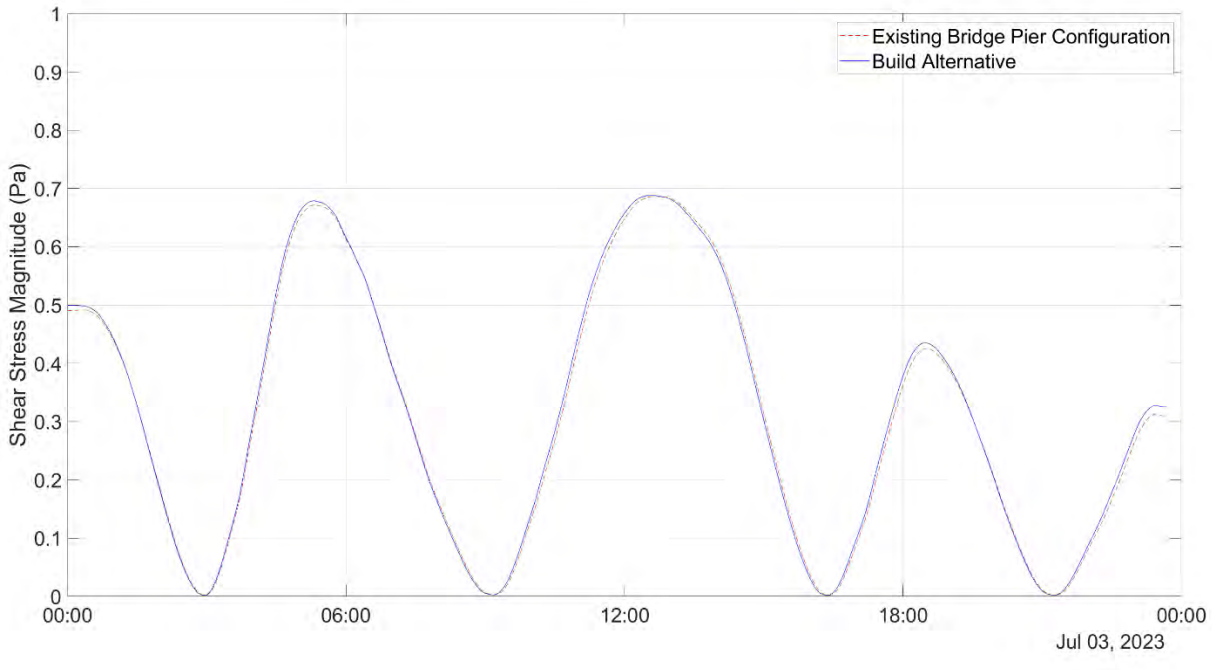


Figure 21 Time series comparison of shear stress at a point within the main channel (Observation Point 2) for existing and Build Alternative C pier configuration in future conditions.

4.2 Potential Impacts to Sediment Transport

Analysis of modeled shear stress between existing and Build Alternative C conditions indicates that there would likely be areas of increases in shear stress primarily within the immediate vicinity of bridge piers. The piers modify near-bed flow velocities, turbulence, and shear stresses, leading to changes in sediment deposition and erosion patterns. Due to bridge configuration differences where the existing and Build Alternative C condition piers do not align, velocity changes are indicative of reduced obstructions where piers are removed and increased obstructions where piers are added.

Cohesive bottom sediments dominate much of the Bay floor in the vicinity of the main channels near the bridge (**Figure 22**). These sediments consist primarily of silt- and clay-sized particles, often mixed with organic material, and exhibit bonding due to consolidation and biological processes. As a result, their erosion behavior differs fundamentally from that of noncohesive sediments such as sand. For cohesive sediments, the critical shear stress varies depending on sediment properties and bed condition, particularly degree of consolidation, clay content, bulk density, water content, and biological binding. Reported critical shear stress values for typical cohesive muds typically range from approximately 0.5 to 1.0 Pa for consolidated beds and 1.0 to 2.0 Pa or greater for well-consolidated or stiff cohesive sediments.

Following bridge construction, localized changes in sediment composition are expected in response to the altered hydraulic conditions around new and modified pier foundations. Increased near-bed shear stresses and turbulence adjacent to piers may initially promote transport of fine cohesive material or redistribution of surficial sediments within pier scour zones. Conversely, areas where obstructions are removed or flow is locally reduced may experience short-term deposition of finer material. Over time, however, these construction-related disturbances are expected to diminish as cohesive sediments redeposit, consolidate, and adjust to the modified flow field. Therefore, while temporary shifts in sediment composition are anticipated following construction, long-term conditions are expected to reach an equilibrium similar in character to existing sediment distributions.

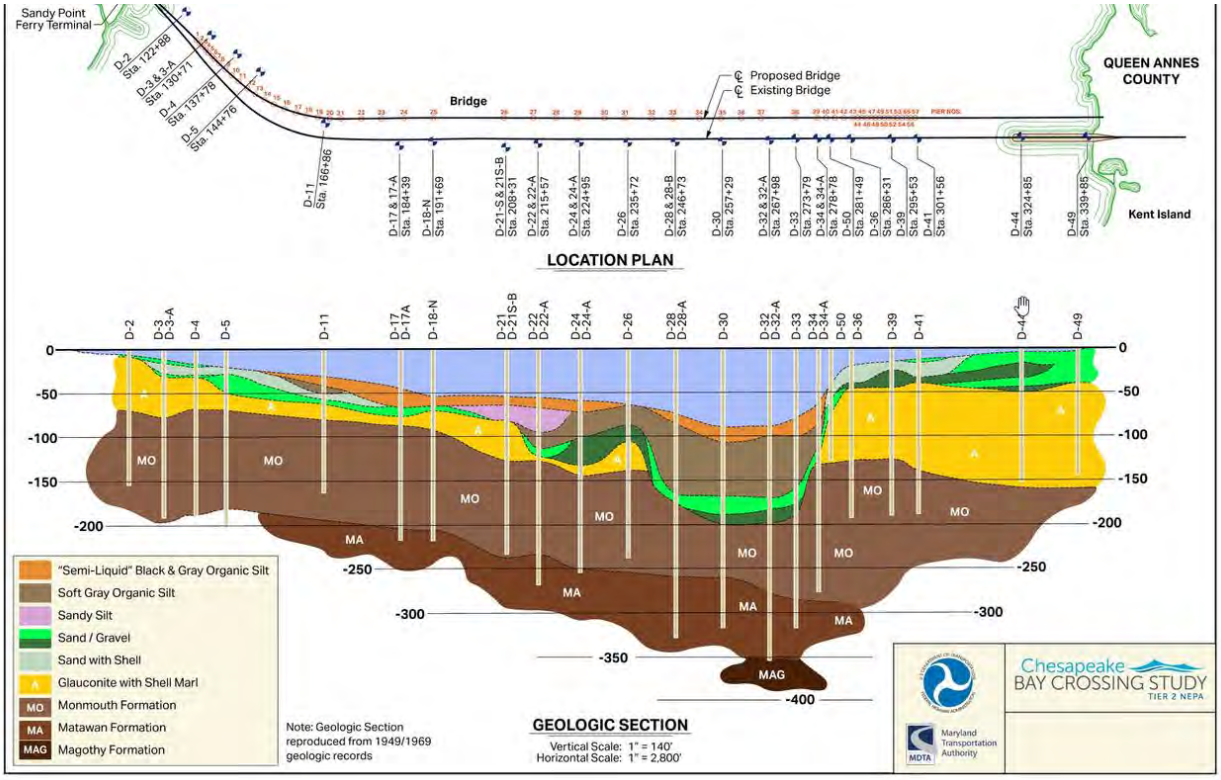


Figure 22. Mapped sediment layers

4.3 Duration of Impact

The duration of potential hydrodynamic impacts was evaluated by examining the cumulative amount of time during which modeled flow velocities and bottom shear stresses exceeded critical thresholds associated with sediment mobilization. Critical velocity and shear stress thresholds representative of sediment erosion in the study area were used as benchmarks for assessing exceedance duration using modeled time series at representative locations near the bridge.

Time series results indicate that exceedance of critical velocity and critical shear stress values occurs only during short intervals associated with peak tidal flows (< 1 hour). For existing bridge conditions under present day water levels, modeled velocities exceed the critical threshold primarily during peak flood conditions. Under the Build Alternative C configuration, exceedance durations are similar in magnitude, with velocities exceeding the critical threshold for approximately one half hour per tidal cycle at locations within 0.3 miles of the bridge piers. For most of each tidal cycle, modeled velocities and shear stresses remain below critical thresholds for both scenarios.

Comparison of existing and Build Alternative C conditions indicates that the Build Alternative C configuration does not result in a meaningful increase in the total duration of time during which critical velocity or shear stress thresholds are exceeded. While localized exceedances near bridge piers may persist slightly longer under Build Alternative C conditions, these differences are limited and do not represent sustained erosive conditions. Beyond the immediate bridge vicinity, exceedance durations are comparable between scenarios.

4.4 Summary

This hydrodynamic modeling analysis was conducted to evaluate potential changes in circulation patterns, flow velocities, and near bed forcing associated with existing and proposed bridge configurations at the Bay Bridge. A three-dimensional Delft3D Flexible Mesh model was developed to simulate tidal currents, wind forcing, and river discharge under present day and future water level conditions. The modeling approach focused on comparing relative differences between existing and proposed conditions using consistent external forcing, allowing hydrodynamic changes attributable to structural modifications.

Analysis of modeled velocity magnitude differences between existing and Build Alternative C conditions in the hydrodynamic model developed to evaluate impacts on the Bay bottom from the placement of new bridge piers (Natural Environmental Technical Report, Appendix F) indicates that there would be areas of increases in near-bed velocity primarily within the immediate vicinity of bridge piers if the span widths are decreased. The piers modify flow velocities and shear stresses, leading to potential changes in sediment transport and deposition. Peak velocities and shear stresses occur during short periods associated with peak tidal flows and are concentrated within the main navigation channel. Outside of the bridge corridor, modeled hydrodynamic conditions under proposed configurations are similar to existing conditions, with differences diminishing rapidly with distance from the bridge. Localized increases in exceedance duration near piers are limited and do not represent sustained forcing capable of driving continuous erosion.

The pier footprints used in the model represent conservative limits of disturbance associated with the conceptual design and were selected as a worst-case representation of the proposed alternative. Actual constructed pier foundations are expected to be smaller than those represented in the model, indicating that the modeled results likely overestimate potential impacts. Resuspension and downstream transport may alter the sediment composition, leading to shifts from coarser to finer substrates, or vice versa, in the vicinity of the structures.

5 REFERENCES

Sweet, William V., Ben D. Hamlington, Robert E. Kopp, Cheryl P. Weaver, Patrick L. Barnard, David Bekaert, William Brooks, et al. 2022. *Global and Regional Sea Level Rise Scenarios for the United States: Updated Mean Projections and Extreme Water Level Probabilities Along U.S. Coastlines*. NOAA Technical Report NOS 01. National Oceanic and Atmospheric Administration.